Available online at www.sciencedirect.com
ScienceDirect
Ocean Engineering 34 (2007) 426–435
OCEAN ENGINEERING
www.elsevier.com/locate/oceaneng

On local and convective accelerations in steep wave events

Atle Jensen*, Didier Clamond, Morten Huseby[1], John Grue

Mechanics Division, Department of Mathematics, University of Oslo, Norway

Received 1 November 2005; accepted 15 March 2006
Available online 3 July 2006

Abstract

The local and convective accelerations of steep irregular wave events have been investigated. These properties are measured by a two-camera PIV technique. Furthermore, the experiments are compared with two different theories including a fully nonlinear and a simplified analytical model. An important result is that the convective term is of the same order of magnitude and of opposite sign as the local acceleration. The convective acceleration term can therefore not be neglected in acceleration and force estimates.

Keywords: Water waves; Accelaration; PIV

1. Introduction

Wave forces on offshore installations can be estimated using Morison's equation (Morison et al., 1950). Velocities and accelerations are needed as a part of the force prediction. In this paper we present measurements of local and convective acceleration in steep wave events recorded from six different irregular seas generated in a wave tank. Velocity fields are obtained by the particle image velocimetry (PIV) technique and presented as a part of the extensive study of local kinematics in Grue et al. (2003). Herein, the particle acceleration of the steepest waves will be presented. Furthermore, the experiments are compared with two different theories including a fully nonlinear and a simplified analytical model. Experimental acceleration fields are extracted from two subsequent velocity measurements using a post-processing technique with high accuracy, see Jensen and Pedersen (2004).

The dynamics of steep irregular waves are often reported from experiments conducted with Laser Doppler methods, which are measuring the velocity/acceleration at a point location. Zelt et al. (1995) has done a study of the local accelerations in irregular waves using Laser Doppler Velocimetry (LDV) and compared to the Wheeler (1970) stretching model. Their motivation was that the local acceleration in irregular waves is proportional to the inertia loading term on large volume structures. Swan et al. (2002) are looking at particle acceleration in an irregular wavetrain using LDA. They measure profiles beneath the crest and compare with a fully nonlinear unsteady wave model. The focus of this paper was to show how to calculate the inertia forces acting on a vertical cylinder.

The advantage of PIV over single point measurements is that the entire velocity field in the section of the fluid is measured. There are few studies on the measurement of acceleration fields. The measurement of accelerations is difficult because it involves the difference between two velocity fields, at slightly different times, both of which are subject to random noise. Due to the small difference between the velocity fields, the relative error is then dramatically increased. In a very brief paper, Chang and Liu (1998) give some estimates of accelerations in an overturning jet. Jakobsen et al. (1997) describe the techniques for measuring accelerations with PIV and give some analysis of the errors which occur using this technique. They claim to be able to measure accelerations to within 3–7%. Jensen et al. (2001) used a two-camera system for measuring the local accelerations in Stokes waves. The measurements of accelerations in short-crested waves gave the best results with relative standard deviations down to 2%.

*Corresponding author.
E-mail address: atlej@math.uio.no (A. Jensen).
[1]Present address: Norwegian Defence Research Establishment (FFI), P.O. Box 25, 2027 Kjeller, Norway.

0029-8018/$ - see front matter © 2006 Elsevier Ltd. All rights reserved.
doi:10.1016/j.oceaneng.2006.03.013

The present paper gives a description of the acceleration fields in steep irregular waves. It is complementary to the paper by Grue et al. (2003) who reported the velocity fields under the crest of 62 steep wave events. The purpose of the present paper is to present acceleration measurements from laboratory simulations and compare them with high-accuracy wave models. All results are non-dimensionalized with respect to the acceleration of gravity, g. Section 2 will present the experimental set-up, Section 3 will discuss the wave models, Section 4 shows results and Section 5 will give a short analysis of the theoretical results.

2. Experiments

The experiments were carried out in a wave tank in the Hydrodynamics Laboratory at the University of Oslo. The tank is 24.6 m long and 0.5 m wide with water depth $h = 0.72$ m. At one end of the tank there is a hydraulic piston wavemaker with movements controlled by a computer and at the other end there is an absorbing beach which reflects less than 3% of the amplitude of the incoming waves.

The acceleration data are obtained by employing an extended PIV system described in Jensen et al. (2001). The system consists of two 1 k × 1 k CCD cameras, a CW Arg-Ion laser and a synchronizer.

The wave elevation of the actual wave field was measured at specified locations using wave gauges. Individual large wave events were identified from these records. Each experiment was repeated, measuring the velocity and acceleration fields under the large wave(s) using PIV. The system was triggered at the instant when the wave crest was in the middle of the field of view (FOV). Three repetitions with the same wave conditions were performed. The water was seeded with polyamid particles with a diameter of approximately 50 μm. The FOV was $25 \times 20\,\mathrm{cm}^2$ and the distance from the wavemaker to $(0, 0)$ in the FOV was 814.5 cm. In all experiments an interrogation window of 64×64 pixels with an overlap of 50% was used. More details of the PIV system and the data processing procedures may be found in Jensen et al. (2001).

The 'local' acceleration field $\partial \boldsymbol{v}/\partial t$ is estimated from the velocity field at two different times, i.e.,

$$\frac{\partial \boldsymbol{v}}{\partial t} \approx \frac{\boldsymbol{v}(\boldsymbol{r}, t_2) - \boldsymbol{v}(\boldsymbol{r}, t_1)}{t_2 - t_1}. \tag{1}$$

The acceleration field $\mathrm{D}\boldsymbol{v}/\mathrm{D}t$ is estimated using the implicit expression

$$\boldsymbol{r}_2 \approx \boldsymbol{r}_1 + \tfrac{1}{2}(t_2 - t_1)[\boldsymbol{v}_1(\boldsymbol{r}_1) + \boldsymbol{v}_2(\boldsymbol{r}_2)], \tag{2}$$

that is solved for $\boldsymbol{r}_2$ and then

$$\frac{\mathrm{D}\boldsymbol{v}}{\mathrm{D}t} = \frac{\boldsymbol{v}(\boldsymbol{r}_2, t_2) - \boldsymbol{v}(\boldsymbol{r}_1, t_1)}{t_2 - t_1}, \tag{3}$$

see Jensen et al. (2003) and Jensen and Pedersen (2004). This corresponds to a simple tracing of pseudo-particles.

The wave events are characterized by the local period and the local maximum elevation, both obtained from the wave gauge measurements, as described in Grue et al. (2003). All the experiments are compared with fully nonlinear solution and a pseudo-third-order Stokes theory.

3. Theory vs. experiments

We expose herein some well-known theoretical results that are the basis for our investigations. Most of this material has been presented in Grue et al. (2003), but are also presented here for completeness.

3.1. Model A—fully nonlinear simulation of the acceleration field in unsteady waves

We performed fully nonlinear simulations of unsteady flows. In particular, we simulate freak waves appearing in wave packets on deep water. The scheme employed is described in Clamond and Grue (2001). The methodology is briefly described here.

First, we compute an exact steady Stokes wave (Fenton, 1988), with wavenumber k and amplitude a (a is half the total wave height). The surface elevation and the tangential velocity at the surface are then multiplied by the 'bell' function

$$\mathrm{sech}[\sigma\sqrt{2}ak^2(x - x_0)], \tag{4}$$

where the parameter σ gives the length of the packet. The case $\sigma = 1$ corresponds to an exact solution of the nonlinear Schrödinger equation. If σ is small enough (i.e., long packet) several envelope solitons appear and interact, creating large waves (freak waves) up to three times larger than the initial carrier wave. More details of this simulation can be found in Clamond and Grue (2002).

Let $\{x; y; t\}$ denote the horizontal, upward vertical and temporal variables, respectively. The still level is at $y = 0$ and the free surface is at $y = \zeta$. Let ϕ be the velocity potential such that $\phi \to 0$ as $y \to -\infty$. The velocity and acceleration fields, from the quantities at the surface obtained by the numerical scheme mentioned above, are computed via the Cauchy integral formula. Indeed, the velocity field—i.e., $w(z, t) = \phi_x - \mathrm{i}\phi_y = u - \mathrm{i}v$ with $z = x + \mathrm{i}y$—being a holomorphic function, as its derivatives, we have

$$w = \frac{1}{2\mathrm{i}\pi}\oint_{\partial D}\frac{w(z', t)}{z' - z}\,\mathrm{d}z', \quad w_z = \frac{1}{2\mathrm{i}\pi}\oint_{\partial D}\frac{w(z', t)}{(z' - z)^2}\,\mathrm{d}z',$$
$$w_t = \frac{1}{2\mathrm{i}\pi}\oint_{\partial D}\frac{w_t(z', t)}{z' - z}\,\mathrm{d}z', \tag{5}$$

where $z' \in \partial D$ and $z \in D$ for some domain D. Once these quantities have been computed, the acceleration field is given by

$$\frac{\mathrm{D}w}{\mathrm{D}t} = \frac{\partial w}{\partial t} + w^*\frac{\partial w}{\partial z}, \tag{6}$$

where the asterisk denotes the complex conjugate.

3.2. Model B—third-order Stokes theory

Another analytical reference is Stokes third-order theory. We consider a periodic progressive irrotational surface wave motion in deep water. Denoting by $\{g;\omega\}$ the acceleration due to gravity and the angular frequency, the very well-known Stokes third-order approximation can be formulated as

$$k\sqrt{k/g}\phi = \varepsilon e^{ky}\sin\theta + O(\varepsilon^4), \tag{7}$$

$$k\zeta = (1+\tfrac{1}{8}\varepsilon^2)\varepsilon\cos\theta + \tfrac{1}{2}\varepsilon^2\cos 2\theta + \tfrac{3}{8}\varepsilon^3\cos 3\theta + O(\varepsilon^4), \tag{8}$$

$$\omega/\sqrt{gk} = 1 + \tfrac{1}{2}\varepsilon^2 + O(\varepsilon^4), \tag{9}$$

with $\theta = kx - \omega t$ and where the 'small' parameter ε is related to the maximum of the surface elevation by

$$k\zeta_m = \varepsilon + \tfrac{1}{2}\varepsilon^2 + \tfrac{1}{2}\varepsilon^3 + O(\varepsilon^4). \tag{10}$$

Note that ε is the amplitude of the fundamental frequency of the velocity potential at $y = 0$. The estimated wave slope $\frac{1}{2}kH$ (H the total wave height) is related to ε by $\frac{1}{2}kH = \varepsilon + \frac{1}{2}\varepsilon^3$.

From the approximations (7)–(9) the velocity field is given by

$$\sqrt{\frac{k}{g}}\frac{\partial\phi}{\partial x} \simeq \varepsilon e^{ky}\cos\theta, \quad \sqrt{\frac{k}{g}}\frac{\partial\phi}{\partial y} \simeq \varepsilon e^{ky}\sin\theta, \tag{11}$$

the local part of the acceleration field by

$$\frac{1}{g}\frac{\partial\phi_x}{\partial t} \simeq \left(1+\frac{1}{2}\varepsilon^2\right)\varepsilon e^{ky}\sin\theta,$$
$$\frac{1}{g}\frac{\partial\phi_y}{\partial t} \simeq -\left(1+\frac{1}{2}\varepsilon^2\right)\varepsilon e^{ky}\cos\theta \tag{12}$$

and the acceleration field (i.e., local plus convective terms) by

$$\frac{1}{g}\frac{D\phi_x}{Dt} \simeq \left(1+\frac{1}{2}\varepsilon^2\right)\varepsilon e^{ky}\sin\theta,$$
$$\frac{1}{g}\frac{D\phi_y}{Dt} \simeq -\left(1+\frac{1}{2}\varepsilon^2\right)\varepsilon e^{ky}\cos\theta + \varepsilon^2 e^{2ky}. \tag{13}$$

3.3. Measurements on non-dimensional form

We shall now direct our attention to the vertical acceleration below the crest. For Stokes third-order waves the scaled dimensionless acceleration appears as follows (see Eq. (13)):

$$A = \frac{1}{\varepsilon + 1/2\varepsilon^3}\frac{1}{g}\frac{D\phi_y}{Dt}\bigg|_{\theta=0} = -e^{ky} + \varepsilon e^{2ky} + O(\varepsilon^3). \tag{14}$$

The quantity A provides a unified reference for the exact vertical acceleration. However, A has not exactly a self-similar profile (i.e., A depends on ε). To investigate the relative effects of the local and convective terms, we define a reference for the local acceleration,

$$A_L = \frac{1}{\varepsilon + 1/2\varepsilon^3}\frac{1}{g}\frac{\partial\phi_y}{\partial t}\bigg|_{\theta=0} = -e^{ky} + O(\varepsilon^3) \tag{15}$$

and a reference for the nonlinear convective term

$$A_C = \frac{1}{\varepsilon^2 + 1/2\varepsilon^4}\frac{1}{g}\left[\frac{D\phi_y}{Dt} - \frac{\partial\phi_y}{\partial t}\right]_{\theta=0} = e^{2ky} + O(\varepsilon^2). \tag{16}$$

These quantities are related by $A = A_L + \varepsilon A_C$.

The interesting feature of A_L and A_C is their independence of the wave slope (self-similarity) up to a certain order of ε. Thus, by measuring these quantities for various 'real' waves, we shall investigate their 'universality'.

Scaling of experimental accelerations in unsteady waves may be obtained in a similar way. The important step is to define local wave parameters with values of ω, k and a. This procedure has been found efficient to characterize the under-crest kinematics of steep transient waves (Grue et al., 2003). The same procedure is then applied to investigate the under-crest dynamics of steep unsteady waves. The practical methodology is briefly explained herein (see also Grue et al., 2003).

As the relations (15) and (16) show, an appropriate scaling leads to an (almost) universal profile under the crest. The scaling involves the local parameters ω, k and ε that have to be determined from the data records. With experimental data obtained by PIV or other means, only a small portion of the wave is measured. It is therefore impossible to apply a Fourier transform to calculate k or ε. On the other hand, it is very easy to measure the maximum

Table 1
Properties of the different irregular wave series using the JONSWAP spectrum

Series	H_s (cm)	T_p (s)	$\omega_p^2 H_s/2g$	ak	f (s^{-1})	kh
I	6.55	0.939	0.15	0.19–0.34	1.21–1.30	3.9–4.6
II	9.60	1.150	0.15	0.21–0.34	0.96–1.04	2.4–2.9
III	8.00	1.150	0.12	0.14–0.34	0.82–1.19	1.6–3.7
V	5.45	0.939	0.12	0.26–0.40	1.14–1.41	3.5–4.9
VI	6.55	1.040	0.12	0.18–0.31	1.01–1.29	2.9–4.4
IV	6.67	1.150	0.10	0.17–0.22	0.98–1.22	2.7–4.2

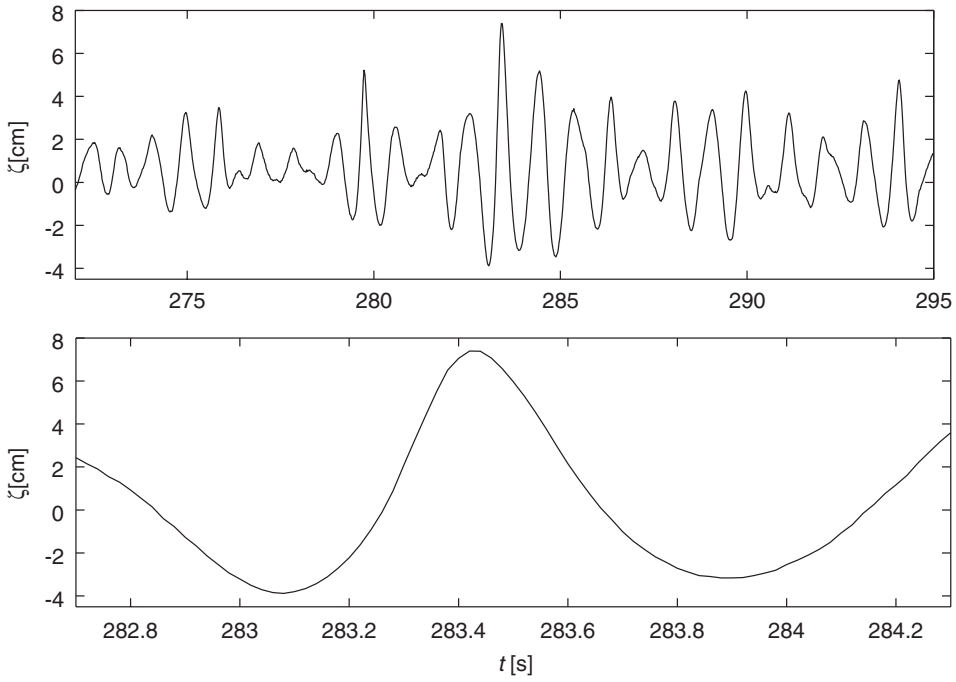

Fig. 1. Upper panel: JONSWAP spectrum with $H_s = 0.065$, $T_1 = 0.78$ and $\gamma = 3.3$. Lower panel: enlarged subsection from upper panel. The position corresponds to $x = 0$ in Fig. 4(b) and is 814.5 cm from the reference position of the paddle.

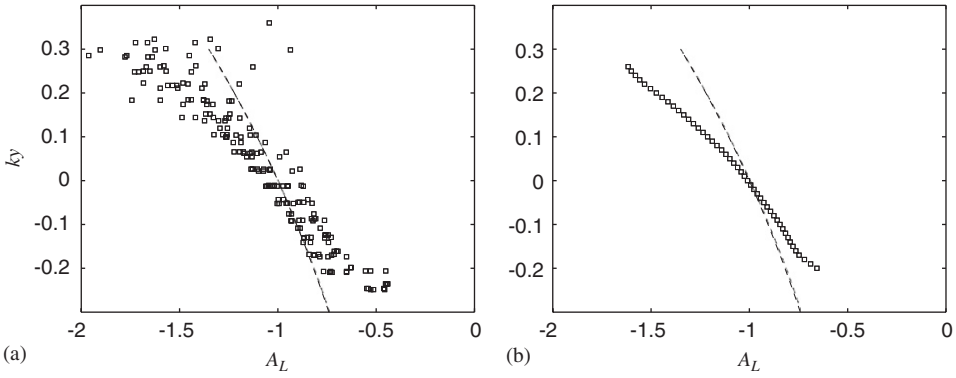

Fig. 2. Left panel: linear term for all non-breaking waves, compared to Stokes third-order theory (dashed lines). Measurements are shown as symbols. Right: symbols are the mean of all measurements.

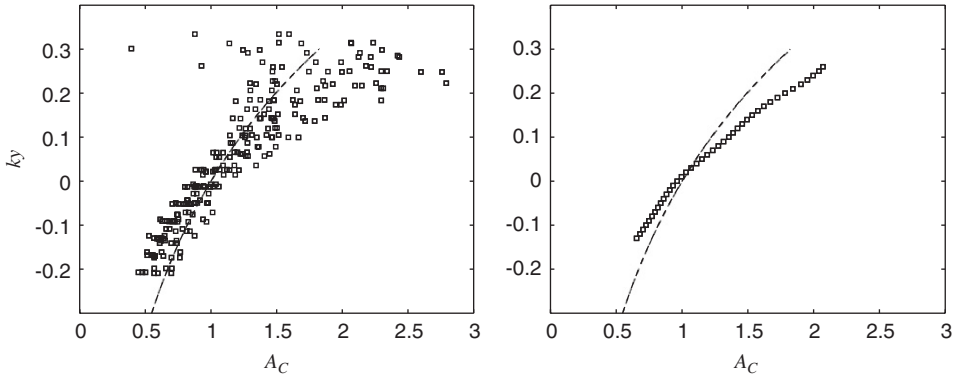

Fig. 3. Left panel: nonlinear convective term for all non-breaking waves, compared to Stokes third-order theory (dashed lines). Right: symbols are the mean of all measurements.

elevation ζ_m and a local trough-to-trough period T_{TT} of a large wave event. A local angular frequency is then defined by $\omega = 2\pi/T_{TT}$, the local wavenumber k and the local 'steepness' ε are derived solving numerically the set of equations (9)–(10).

4. Results

The steepest wave events in an irregular sea are investigated, $0.30 < \varepsilon < 0.41$. The sea states were produced in the wave tank using a JONSWAP spectrum, see e.g., Gran (1992) and Hasselmann et al. (1973). It is characterized by the significant wave height, H_s, the peak period, T_p, of the spectrum, and the peak enhancement factor $\gamma = 3.3$. A total of six different time series were produced.

The ranges of the wave slope, $\varepsilon = ak$, inverse period, f, and wavenumber of the individual waves times the water depth, kh, are indicated in Table 1 (where $\omega_p = 2\pi/T_p$).

In Fig. 1 the upper panel shows the elevation measurement of the irregular wavetrain (series 1). The lower panel shows a steep wave event, where the dynamics are presented in Fig. 4(b).

By using the theoretical references (15) and (16) all experiments are compared with A_L and A_C. Herein, the results are independent of ε. Fig. 2(a) shows the local vertical accelerations compared with $-e^{ky}$, only the

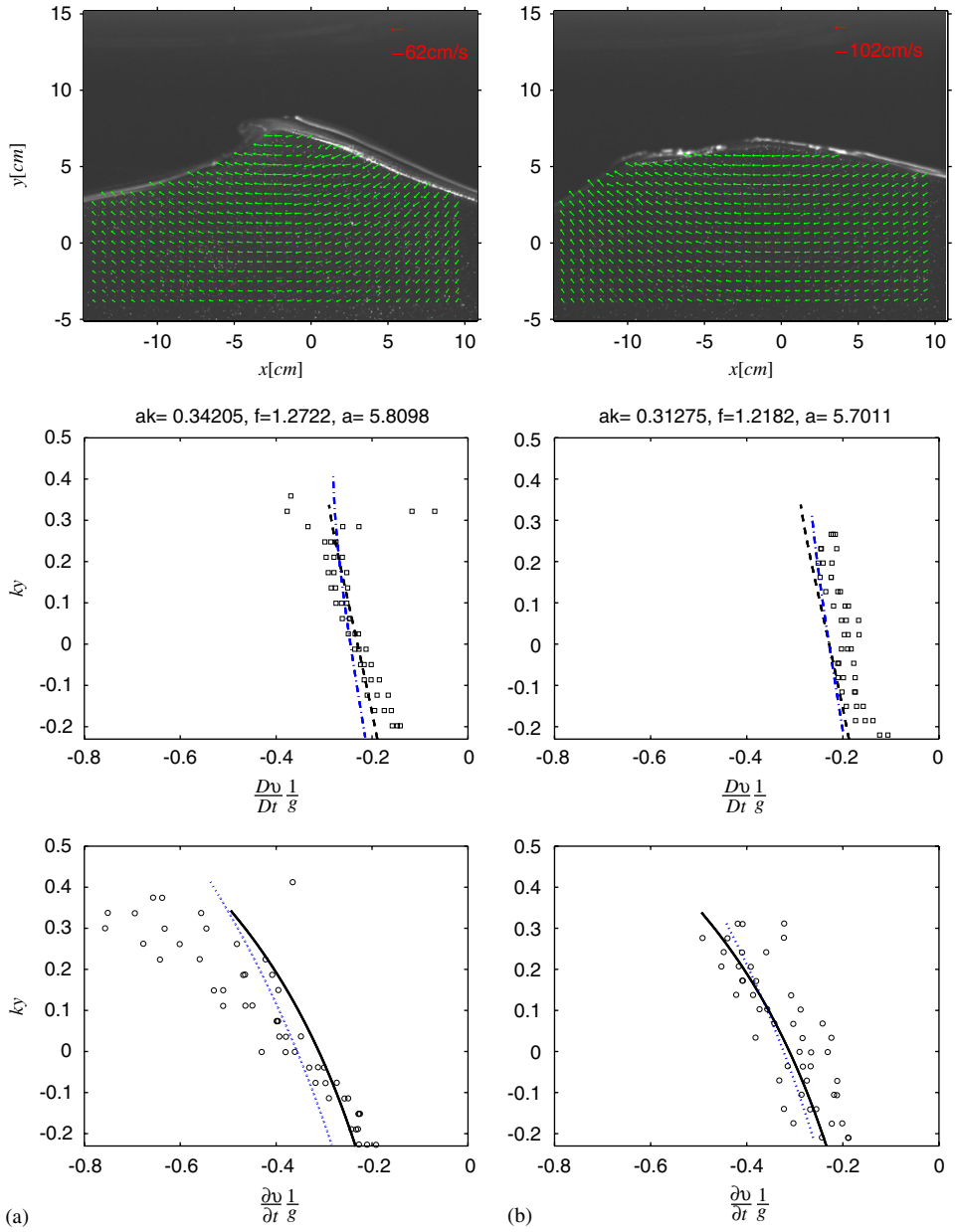

Fig. 4. Series 1, (a) Left panels: $ak = 0.34$ and $kh = 4.2$. (b) Right panels: $ak = 0.31$ and $kh = 3.9$. Local acceleration: solid is fully nonlinear simulation (model A), dots is simplified analytical model (model B) and circles are experiments. Particle acceleration: dashed is model A, dashdots is model B and squares are experiments. Top figures are PIV images with velocity vector field.

non-breaking waves are presented in the figure. Fig. 3(a) shows the convective part of the vertical accelerations compared to e^{2ky}. Figs. 2(b) and 3(b) show the difference between the mean of all experiments and the theoretical reference, the maximum deviation is 23% for both the linear and convective accelerations. The scatter is somewhat large but it gives a quantitative view of the comparison. It must be noted that the experimental waves are affected by several irregular motions in the tank due to the long series that has been run, e.g long waves and currents, but overall the agreement is good. When combining PIV and acceleration less accuracy is expected, see Jensen and Pedersen (2004) and Jensen et al. (2001).

Figs. 4–7 show the vertical acceleration profile under the crest, both local and particle accelerations, non-dimensionalized by g. The fully nonlinear theory profiles are the same in all figures with local wavenumber, $\varepsilon = 0.29$. In Fig. 4(a) the wave is spilling but it still compares well with the different theories. The maximum acceleration is $-0.8g$ for A_L in the experiments and A is $-0.3g$. It should be noted that linear theory over-predicts the acceleration by 50%. Fig. 4(b) is less steep but a closer collapse of data points is seen. These two events have local wave slope of $\varepsilon = 0.34$ and 0.31, respectively ($kh = 4.2$ and 3.9).

In Fig. 5(a) ($\varepsilon = 0.34$, $kh = 2.4$, series 2) the wave breaks and the scatter in the experimental data are unavoidable. The non-breaking wave in Fig. 5(b) is much

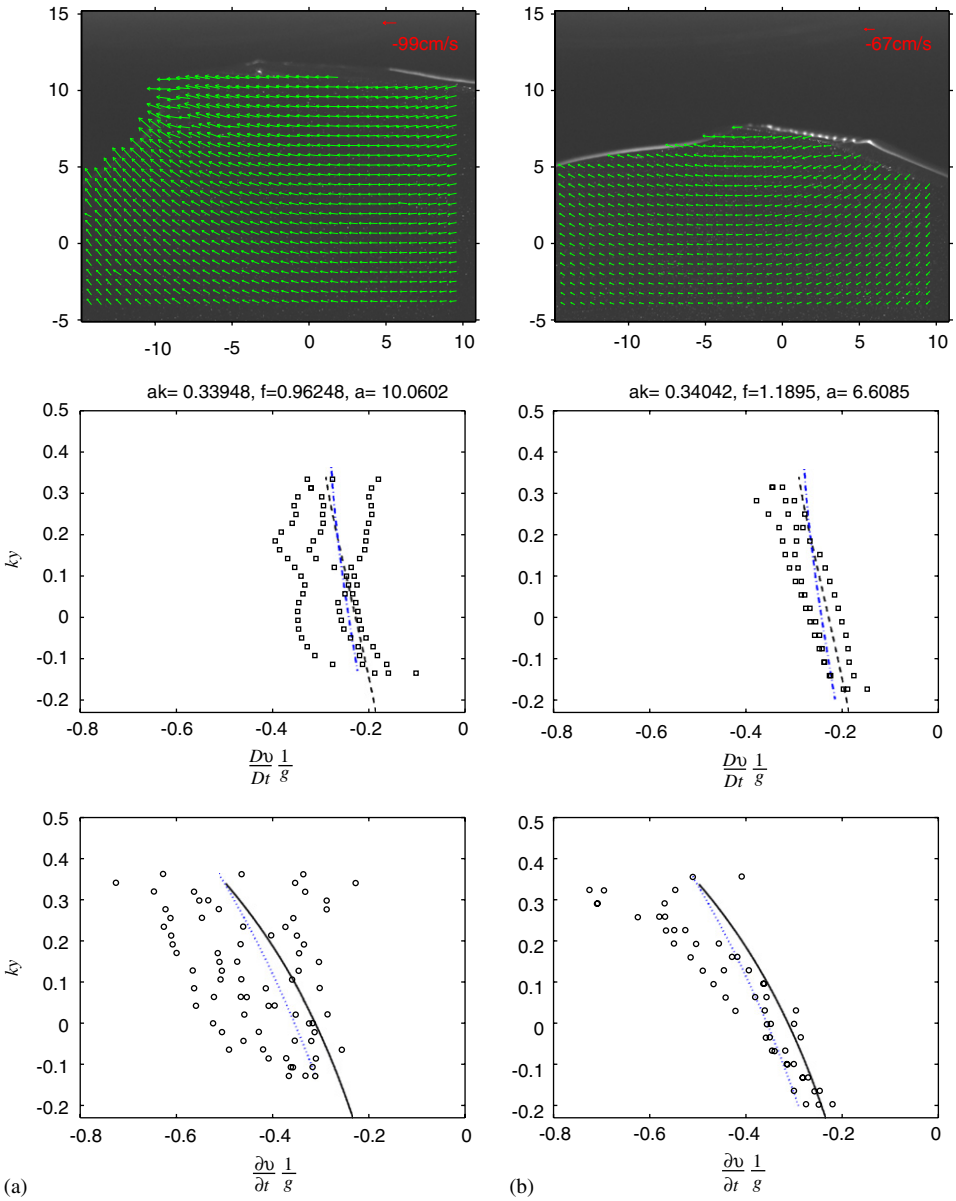

Fig. 5. (a) Left panels: series 2, $ak = 0.34$ and $kh = 2.4$. (b) Right panels: series 3, $ak = 0.34$ and $kh = 3.7$. Local acceleration: solid is fully nonlinear simulation (model A), dots is simplified analytical model (model B) and circles are experiments. Particle acceleration: dashed is model A, dashdots is model B and squares are experiments. Top figures are PIV images with velocity vector field.

cleaner and with higher A_L than the theories. $\varepsilon = 0.34$ ($kh = 3.7$, series 3) and compared to Fig. 4(a) the features of the profiles are similar.

The waves from series 5 are the steepest ones in these series of experiments. Fig. 6(a) ($ak = 0.31, kh = 4.4$) compares well with the different theories. The wave close to breaking in Fig. 6(b) ($ak = 0.41$, $kh = 5.0$) has larger scatter in the experimental data, as expected. But the profiles indicate the same as the other wave events.

Series 6 (Fig. 7(a)) ($ak = 0.31$, $kh = 3.2$) breaks and the PIV method have difficulties with extracting velocities near the surface. But further down it compares very well. Fig. 7(b) ($ak = 0.31$, $kh = 4.5$) has somewhat the same results as the latter, but the repeatability is higher due to non-breaking.

5. Analysis of the theoretical results

We proceed with the numerical results as for the experimental data: the wave characteristics are extracted from temporal evolutions at one point. We consider the largest waves only. The different waves are extracted from significantly different times and are thus not correlated. It is worth noting that the waves investigated here have been extracted systematically from the files without 'human interaction', i.e., we did not select only waves that support our claim.

As for the Stokes wave, the differences between the exact acceleration and its linear approximation is large (Fig. 8). Both the linear and convective parts of the acceleration fit well with the exponential profiles (Fig. 9).

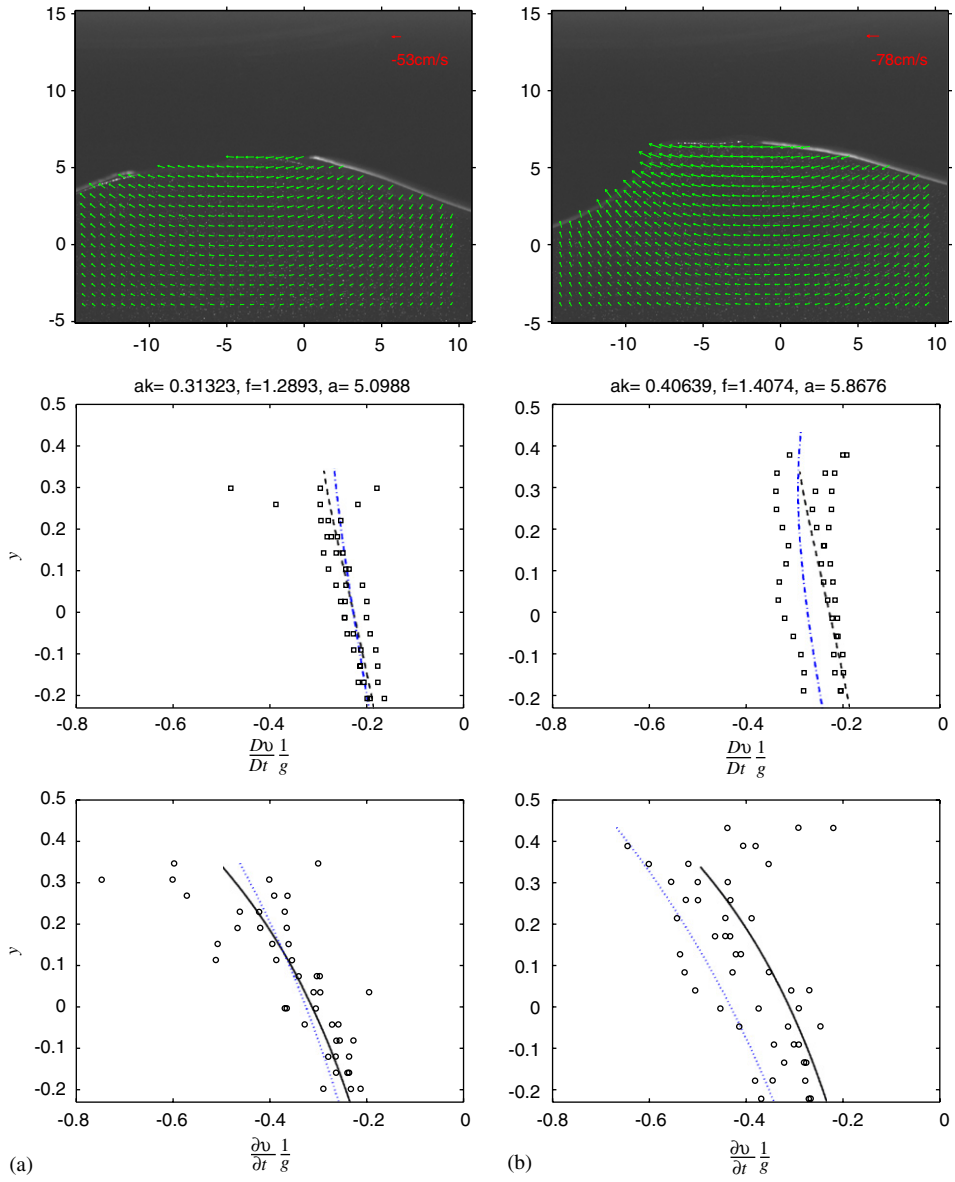

Fig. 6. Series 5, (a) Left panels: $ak = 0.31$ and $kh = 4.4$. (b) Right panels: $ak = 0.41$ and $kh = 5.0$. Local acceleration: solid is fully nonlinear simulation (model A), dots is simplified analytical model (model B) and circles are experiments. Particle acceleration: dashed is model A, dashdots is model B and squares are experiments. Top figures are PIV images with velocity vector field.

We observe some 'tilt' in the profiles (compared to the Stokes wave) that is logical since the freak waves are not symmetrical. However, the deviation is small, much smaller than the accuracy that one can expect from data recorded in situ.

We also observe that different waves with similar local characteristics have very similar acceleration profiles. This means that the methodology employed is robust and consistent.

In conclusion, it turns out that the scaled dimensionless acceleration related quantities A_L and A_C are quite universal parameters for freak waves in deep water.

Investigating numerically steeper waves is impossible since these waves break and the computation stops.

6. Concluding remarks

The dynamics of steep irregular wave events has been investigated. A total of six different irregular wave series using the JONSWAP spectrum have been generated in the wave tank. A total of eight waves are measured by a PIV system and compared to two different wave models. Each wavetrain is repeated three times. The focus of the present study is to find the local parameters ω, k and ε, which need to be determined from the data records. The maximum elevation ζ_m and a local trough-to-trough period T_{TT} of a large wave event are measured. A local angular frequency is then defined by $\omega = 2\pi/T_{TT}$, the local wavenumber k and the local 'steepness' ε are derived solving numerically

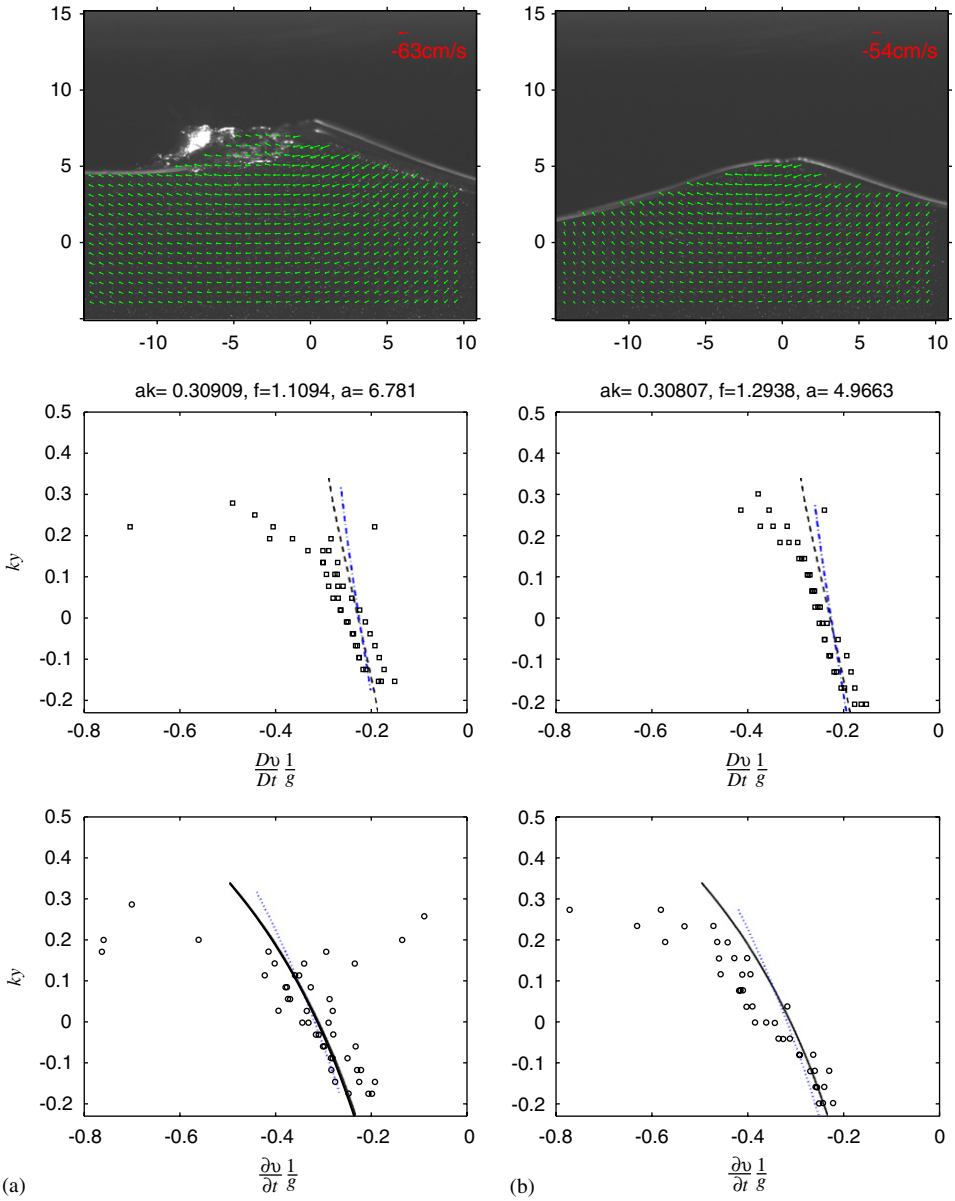

Fig. 7. Series 6, (a) Left panels: $ak = 0.31$ and $kh = 3.2$. (b) Right panels: $ak = 0.31$ and $kh = 4.5$. Local acceleration: solid is fully nonlinear simulation (model A), dots is simplified analytical model (model B) and circles are experiments. Particle acceleration: dashed is model A, dashdots is model B and squares are experiments. Top figures are PIV images with velocity vector field.

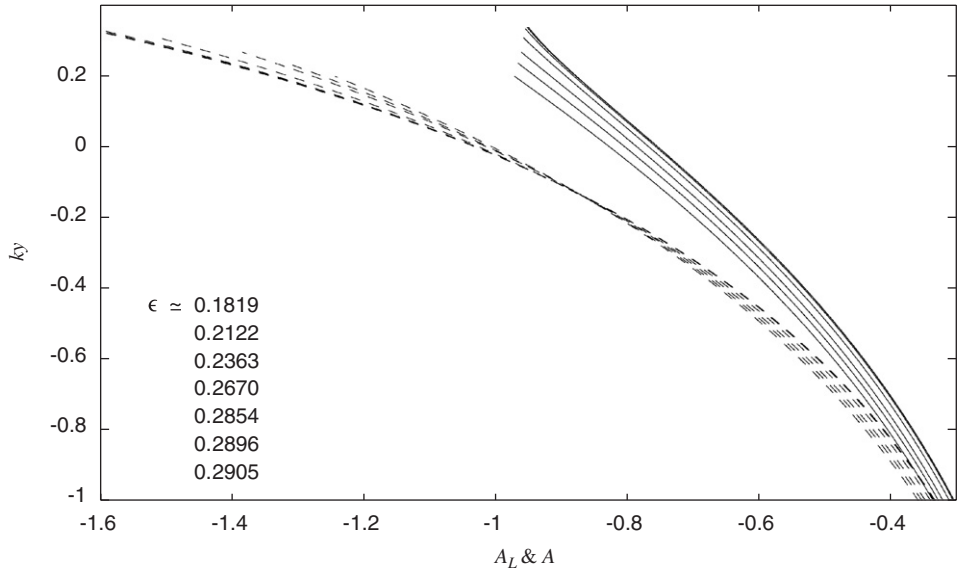

Fig. 8. Particle versus local vertical acceleration under crest of freak waves. Solid lines: particle acceleration A. Dashed lines: local acceleration A_{L}.

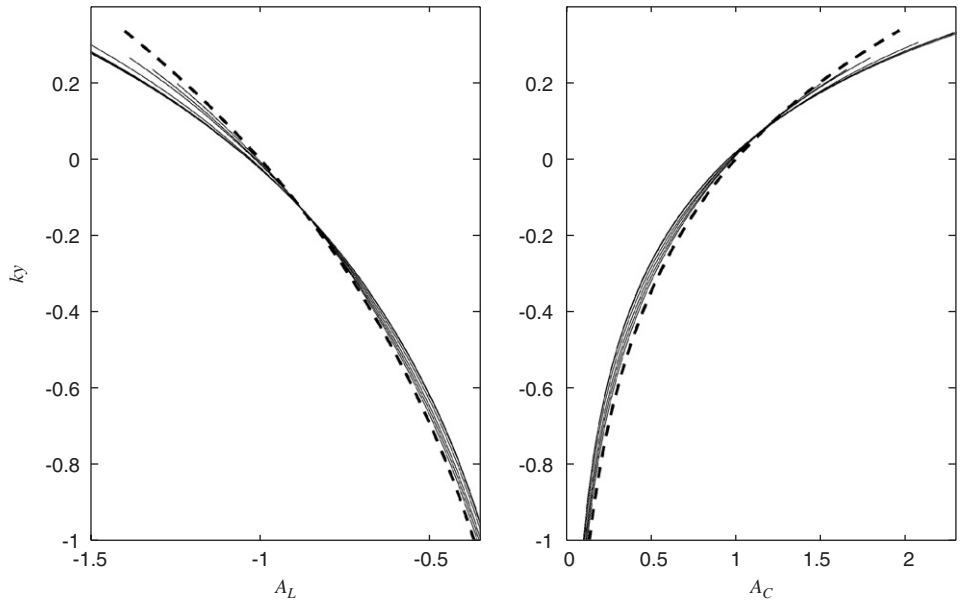

Fig. 9. Local and convective accelerations under crest of freak waves. Solid lines: Fully nonlinear simulation. Dashed lines: $-e^{ky}$ (left), e^{2ky} (right).

the set of equations (9)–(10). The particle acceleration Dv/Dt is found and the maximal vertical accelerations are taken below the crest. This is non-dimensionalized by g and compared to wave models A and B.

By comparing the experiments with (15) and (16) a nice collapse of data is shown in Figs. 2 and 3. The scatter in the experimental results are due to less accuracy which is natural for these types of measurements compared to velocity measurements which are presented in Grue et al. (2003). An important result is that the convective term is of the same order of magnitude and of opposite sign as the local acceleration. The convective acceleration term can therefore not be neglected in acceleration and force estimates.

Looking at several steep wave events locally, a more detailed analysis can be made. It should be noted, as indicated above, that linear theory will over-predict the acceleration by 30% to 50% in all the events that is presented herein.

The fully nonlinear model A shows extremely good agreement compared to the experiments. And there is no doubt about the importance of such simulations. However,

the simple pseudo-wave model B gives also good results and provides relevant complement when a local ε can be extracted from the wave records.

In summary, we have found that

- linear theory over-predicts the vertical acceleration by 50% for the steepest waves;
- all steep wave events compare well with the present theories;
- the maximum elevation ζ_m and a local trough-to-trough period T_{TT} and solving Eqs. (9)–(10) are sufficient to establish the acceleration profile under the crest.

References

Chang, K.-A., Liu, P.L.-F., 1998. Velocity, acceleration and vorticity under a breaking wave. Physics of Fluids 10, 327–329.

Clamond, D., Grue, J., 2001. A fast method for fully nonlinear water-wave computations. Journal of Fluid Mechanics 447, 337–355.

Clamond, D., Grue, J., 2002. Interaction between envelope solitons as a model for freak wave formations. Comptes Rendus de l'Académie des Sciences. Série deux b, Mécanique 330, 575–580.

Fenton, J.D., 1988. The numerical solution of steady water wave problems. Computers and Geosciences 14 (3), 357–368.

Gran, S., A Course in Ocean Engineering. Elsevier, Amsterdam, The Netherlands. (ISBN 0-444-88143-3).

Grue, J., Clamond, D., Huseby, M., Jensen, A., 2003. Kinematics of extreme water waves. Applied Ocean Research 25, 355–366.

Hasselmann, K., et al., 1973. Measurements of wind-wave growth and swell decay during the joint north sea wave project (JONSWAP). Ergänzungsheft zur Deutsche Hydrographische Zeitschrift, Reihe A 8 (12).

Jakobsen, M.L., Dewhirst, T.P., Greated, C.A., 1997. Particle image velocimetry for predictions of acceleration fields and force within fluid flows. Measurement Science and Technology 8, 1502–1516.

Jensen, A., Pedersen, G.K., 2004. Optimization of acceleration measurements using PIV. Measurement Science and Technology 15, 2275–2283.

Jensen, A., Sveen, J.K., Grue, J., Richon, J.-B., Gray, C., 2001. Accelerations in water waves by extended particle image velocimetry. Experiments in Fluids 30, 500–510.

Jensen, A., Pedersen, G.K., Wood, D.J., 2003. An experimental study of wave run-up at a steep beach. Journal of Fluid Mechanics 486, 161–188.

Morison, J.P., O'Brien, M.P., Johnson, J.W., Schaaf, S.A., 1950. The force exerted by surface waves on piles. Petroleum Transactions 189, 149–154.

Swan, C., Bashir, T., Gudmestad, O.T., 2002. Nonlinear inertial loading. Part I: accelerations in steep 2-D water waves. Journal of Fluids and Structures 16 (3), 391–416.

Wheeler, J., 1970. Method for calulating forces produced by irregular waves. Journal of Petroleum Technology, 359–367.

Zelt, J.A., Gudmestad, O.T., Skjelbreia, J.E., 1995. Fluid accelerations under irregular waves. Applied Ocean Research 17, 43–54.